

## NUMERICAL STUDY OF COSMIC RAY DIFFUSION IN MHD TURBULENCE

A. BERESNYAK<sup>1</sup>, H. YAN<sup>2</sup>, A. LAZARIAN<sup>1</sup>

*Draft version June 19, 2018*

### ABSTRACT

We study diffusion of Cosmic Rays (CRs) in turbulent magnetic fields using test particle simulations. Electromagnetic fields are produced in direct numerical MHD simulations of turbulence and used as an input for particle tracing, particle feedback on turbulence being ignored. Statistical transport coefficients from the test particle runs are compared with earlier analytical predictions. We find qualitative correspondence between them in various aspects of CR diffusion. In the incompressible case, that we consider in this paper, the dominant scattering mechanism occurs to be the non-resonant mirror interactions with the slow-mode perturbations. Perpendicular transport roughly agrees with being produced by magnetic field wandering.

*Subject headings:* cosmic rays, scattering, MHD, turbulence

### 1. INTRODUCTION

The interaction between Cosmic Rays, highly energetic charged particles, and astrophysical fluids is mediated by magnetic fields. As magnetic fields are usually turbulent, CRs do not freely stream along these fields but scatter (see, e.g., Schlickeiser 2002). Efficient scattering is essential for a variety of acceleration mechanisms of CRs, such as, for example, diffusive shock acceleration (Krymsky 1977, Bell 1978, Malkov & Drury 2001 and ref. therein).

Understanding MHD turbulence is essential for the correct description of CR propagation. One popular model has been based on the combination of slab and two-dimensional perturbations (see Bieber, Smith, & Matthaeus 1988). Simplicity of this empirical model has appealed to researchers and has been used to account for propagation of CRs in solar wind and magnetosphere. Numerical simulations (see Cho & Vishniac 2000, Maron & Goldreich 2001, Müller & Biskamp 2000, Cho, Lazarian & Vishniac 2002, Cho & Lazarian 2002, 2003), however, do not show slab modes, instead, they show Alfvénic modes that exhibit scale-dependent anisotropy consistent with predictions in Goldreich & Sridhar (1995, henceforth GS95). The scalings of compressible modes is still a subject of debate, although it is suggested that slow mode is passively advected by Alfvén mode (GS95, Lithwick & Goldreich 2001), which was verified by numerics, also fast mode showed relative isotropy which was suggestive of a separate acoustic-type cascade (Cho & Lazarian 2002, 2003).

While particular aspects of the GS95 model, e.g. the value of the spectral index, has been debated (see Boldyrev 2005, 2006, Beresnyak & Lazarian 2006, Gogoberidze 2007, Beresnyak & Lazarian 2009a,b), this model provide a good start for studying CR scattering. This program was realized in a number of publications such as Chandran (2000), Yan & Lazarian (2002, 2004, henceforth YL02, YL04, respectively), Brunetti & Lazarian (2007). In the last three papers, following Cho & Lazarian (2003), MHD turbulence has been decomposed into Alfvén, slow and fast modes.

In a complex problem of propagation and acceleration of CRs we often use so-called diffusive approximation which assume that the particle scatter or gain energy in small steps. In this approximation the local particle dynamics will be averaged to obtain the spatial diffusion coefficient,  $D_{xx}$ , and the momentum diffusion coefficient,  $D_{pp}$ ; that go into the advection-diffusion equation for the evolution of quasi-isotropic CR distribution function  $f$ :

$$\frac{\partial f}{\partial t} + u \frac{\partial f}{\partial x} = \frac{\partial}{\partial x} \left( D_{xx} \frac{\partial f}{\partial x} \right) + \frac{p}{3} \frac{\partial u}{\partial x} \frac{\partial f}{\partial p} + \frac{1}{p^2} \frac{\partial}{\partial p} \left( p^2 D_{pp} \frac{\partial f}{\partial p} \right), \quad (1)$$

(e.g., Skilling 1975). The source terms has been added to the RHS of this equation to account for injection from thermal particles and the proper boundary conditions should be defined. Here we assumed for simplicity that  $f(x, p)$  depends only on one spatial coordinate  $x$  and the magnitude of CR momentum,  $p$ . This equation uses “local” system of reference, where particle momentum is measured with respect to the rest frame of the fluid. In a situation when the advection-diffusion equation is not adequate one has to fall back to more general approaches, such as Vlasov’s equation (see, e.g., Schlickeiser 2002). In this paper we study particle dynamics assuming diffusion approximation and we monitor if this dynamics looks like a diffusive dynamics or not.

The propagation of CRs is a mature quantitative field, which makes use both of analytical studies and numerical simulations. For example, a quasi-linear theory (QLT) was used to calculate scattering of CRs propagating in a mean magnetic field with small perturbations. However, as turbulence paradigms were changing, so were the results of CR scattering theories. The purpose of this paper is to measure CR scattering numerically, based on the best available direct numerical simulations of MHD turbulence and compare these results with what scattering theories predict.

QLT has demonstrated that the gyroresonance in GS95 type turbulence is substantially suppressed and negligible (Chandran 2000, YL02, YL04). However, the key assumption of QLT, that the particle’s orbit is unper-

<sup>1</sup> Astronomy Department, University of Wisconsin, Madison, WI 53706

<sup>2</sup> Astronomy Department, University of Arizona

turbed, significantly limits its applicability. Additionally, QLT has problems in treating scattering of particles with momentum nearly perpendicular to the magnetic field (see Jones, Birmingham & Kaiser 1973, 1978; Völk 1973, 1975; Owens 1974; Goldstein 1976; Felice & Kulsrud 2001) and perpendicular transport (see Kóta & Jokipii 2000, Matthaeus et al. 2003).

Various non-linear theories have been proposed to improve the QLT (see Dupree 1966, Völk 1973, 1975, Jones, Kaiser & Birmingham 1973, Goldstein 1976). In the recent paper of Yan & Lazarian (2008, henceforth YL08), a nonlinear formalism (NLT) based on Völk (1975) was developed. The gyroresonance was found to be marginal in incompressible turbulence. However, transit time damping (TTD) was fairly efficient which is different from the QLT result. TTD due to nonlinear scattering can be understood as a scattering by large-scale magnetic compressions (magnetic bottles formed by slow mode). The ideas on perpendicular diffusion has been dominated by the field line random walk (Jokipii 1966, Jokipii & Parker 1969, Forman et al. 1974). It can be justified in a situation when CRs do not scatter backwards. However, in three-dimensional turbulence, parallel transport is also diffusive, and this can reduce perpendicular transport.

The difference between QLT and NLT has important astrophysical consequences. Indeed, in some phases, such as hot ISM, the fast mode is strongly damped, which leaves only Alfvén and slow modes for scattering. According to the QLT, however, these modes do not provide any significant scattering. This would predict that there are large volumes in the disk of the Galaxy where CRs do not scatter at all, which would question global simulations of propagation of CRs in the Galaxy or halo made without such an assumption. This will also somewhat contradict the isotropy of galactic CRs observed on Earth, because isotropy suggests efficient scattering. Fortunately, NLT corrects this “zero-scattering” QLT prediction, putting a lower limit on the efficiency of CR scattering, thus mitigating contradictions described above.

Test particle simulation has been used to study CR scattering and transport before, see, e.g., Giacalone & Jokipii (1999), Mace et al (2000), Qin et al. (2002). The aforementioned studies, however, used synthetic data for turbulent fields, which have several disadvantages. Creating synthetic turbulence data which has scale-dependent anisotropy with respect to the local magnetic field (as observed in Cho & Vishniac 2000 and Maron & Goldreich 2001) is difficult and has not been realized yet, as far as we know. Also, synthetic data normally uses Gaussian statistics and delta-correlated fields, which is hardly appropriate for description of strong turbulence. In contrast, in this paper we are using the results of direct numerical MHD simulations as the input data for particle scattering simulations.

Another challenging problem is the back-reaction of CRs to the fluid. A particular mechanism for such a process, called streaming instability, has been popular in describing CR scattering since long time ago (see, e.g., Kulsrud & Pearce 1969). In this paper, however, we consider only *test particle* scattering. This describes an important physical limit where CR density is negligibly small and collective effects are unimportant. Although in realistic astrophysical environments CR density is never small and CR pressure is always dynamically important,

the understanding of the *test particle limit* will give us a firm ground for future research into a more general and more difficult problem of mutual interaction of CRs and MHD fluid.

In this paper we study the scattering by the incompressible component of turbulence. If the fast mode is present, however, it will dominate scattering of low energy CRs, as long as the fast mode is not effectively suppressed (YL04). Another very efficient mechanism of scattering is the instability between CR fluid and MHD fluid (see above). It is present, e.g., when there are strong CR gradients that lead to streaming.

In what follows, we discuss numerical methods, including DNS of MHD turbulence and particle tracing technique in § 2. We discuss theoretical expectations for CR scattering in § 3. We provide numerical measurements of scattering in § 4 and measurements of space diffusion in § 5. We discuss our results in § 6.

## 2. NUMERICAL METHODS

In order to trace particle trajectories we were using electromagnetic fields obtained in direct three-dimensional simulations of MHD turbulence. For the purpose of this paper we were using only incompressible simulations for a variety of reasons. First, we wanted to test those predictions of the theory that pertain to incompressible case. Second, the incompressible simulations were performed with pseudospectral code that has explicit dissipation and, unlike finite-difference code has no uncertainties due to numerical dissipation. Also, incompressible simulations have larger inertial range.

### 2.1. DNS of turbulence

We solved incompressible MHD equations,

$$\partial_t \mathbf{w}^\pm + \hat{S}(\mathbf{w}^\mp \cdot \nabla) \mathbf{w}^\pm = -\nu_n (-\nabla^2)^n \mathbf{w}^\pm + \mathbf{f}^\pm, \quad (2)$$

written in terms of Elsasser variables which are defined in terms of velocity  $\mathbf{v}$  and magnetic field in velocity units  $\mathbf{b} = \mathbf{B}/(4\pi\rho)^{1/2}$  as  $\mathbf{w}^+ = \mathbf{v} + \mathbf{b}$  and  $\mathbf{w}^- = \mathbf{v} - \mathbf{b}$ ,  $\hat{S}$  is a solenoidal projection operator,  $\mathbf{f}^\pm$  is Elsasser forcing. These are general equations which can be used for either turbulence with no mean magnetic field (i.e. when the average of  $\mathbf{w}^+ - \mathbf{w}^-$  is zero), or in a presence of such a mean field. In the latter case perturbations of  $\mathbf{w}^+$  can be seen as the waves propagating oppositely to the magnetic field direction. Both Alfvén and pseudo-Alfvén waves propagate with the same velocity  $v_A = B_0/(4\pi\rho)^{1/2}$ .

We used pseudospectral code described in more detail in Beresnyak & Lazarian 2009(a,b) (henceforth BL09a,b). The pseudospectral code solves Eq. 2 as ordinary differential equation in time for each spacial Fourier harmonic, the “pseudo” coming from the fact that nonlinear term is calculated in real space, and then converted back to Fourier space. The dissipation and divergence-free condition for velocity and magnetic field are done with simple algebraic operations in Fourier space. For time integration we use leapfrog which is time-reversible and numerical dissipation is absent, because nonlinear term, calculated in this manner, preserve both energy and cross-helicity. Therefore the only dissipation come from the explicit dissipation term. The turbulence was driven by either independent Elsasser driv-

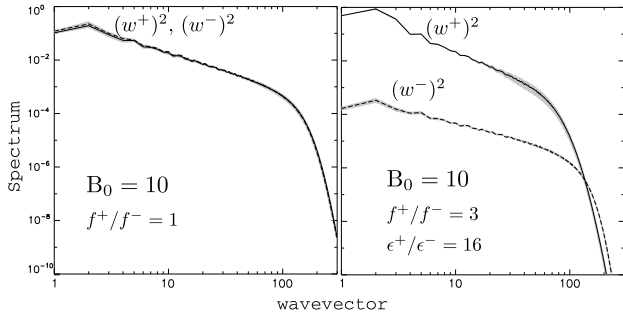


FIG. 1.— Sample spectra from turbulent simulations. Left – balanced case, right – imbalanced case. Shown are Elsasser energy spectra (see BL09a for more details).

ing or by pure velocity driving (which formally corresponds to  $f^+ = f^-$ ). For the purpose of this paper we used the results of 768<sup>3</sup> balanced and imbalanced turbulent simulations from BL09a. Balanced turbulence corresponds to the well-studied limit, where the rms values of  $w^+$  and  $w^-$  are equal. Physically this corresponds to the situation when the flow of  $w^-$  perturbations, which propagate along the mean magnetic field direction, balances the opposing flow of  $w^+$ . The more general case of imbalanced turbulence is less studied (see BL08, BL09a and ref. therein), but more likely to be found in nature. This is due to the fact, that MHD turbulence is often driven by the strong localized source of perturbations and near the source we mostly see waves moving away from the source. Such as a solar wind turbulence near the Sun, which is strongly imbalanced<sup>3</sup>. Naturally, we are also interested in particle scattering in the imbalanced turbulence, although few theoretical predictions of scattering exist in this case, if any.

Another dimension in parameter study of BL09a was the strength of perturbations with respect to the mean field. The  $\delta B \sim B_0$  is called trans-Alfvénic case, where perturbations are of the order of the mean field. We also consider sub-Alfvénic case when perturbations were approximately 10 times weaker than mean field  $B_0$ , which correspond to so called Alfvénic Mach number  $M_A \sim 0.1$ . The latter case can be considered as smaller scales of trans- or super-Alfvénic turbulence that cannot be reached directly by 3D simulations of aforementioned flows. In order for sub-Alfvénic turbulence to be strong<sup>4</sup> it has to be driven anisotropically on its outer scale, which was realized in BL09a,b. The computational box was also elongated in the direction of the mean field, with parallel size 10 times larger than perpendicular size for  $M_A = 0.1$  case. Throughout the paper, when we mention the “box size” and the “outer scale of turbulence” it means perpendicular size, the parallel size is the same for trans-Alfvénic cubes and 10 times larger for sub-Alfvénic

<sup>3</sup> The measurement of the imbalance in the solar wind has been possible with the advent of satellites that independently measure the velocity and the magnetic field at the same point. Similar measurements for other astrophysical sources, such as ISM, are yet to be developed.

<sup>4</sup> Strong MHD turbulence appears naturally as a result of the anisotropic cascade. Even if turbulence is driven weakly with respect to the mean field, the perpendicular cascade of weak turbulence (Galtier et al, 2000) will increase the strength of interaction until it becomes strong. The realistic ISM turbulence, however, is driven strongly, such as  $\delta B \sim B_0$  on the outer scale. So turbulence is strong to begin with and continue to be strong along the cascade (GS95).

cubes.

The note of caution has to be said with regard to sub-Alfvénic simulations being the small scales of trans-Alfvénic turbulence. As we use periodic boundaries, the scales which are larger than the cube size are excluded from consideration. This means that we cut out a range of scales in the inertial interval of turbulence and all larger scales are represented only by the value of the mean magnetic field (the mean velocity can be excluded by the local frame of reference). This could or could not be satisfactory for simulations of particle scattering. If the resonant scattering mechanism is effective, then particles mostly interact with those scales of magnetic perturbations that are present in the simulation. In the opposite case the aforementioned interaction can be less effective than the interaction with large scale perturbations that are not present in the numerical cubes. In this case the result should not be trusted. We will return to this question below. Accidentally, the QLT consider scattering in a manner which is consistent with approach that ignores larger scales and consider particle gyrating along a strong guiding field and interacting with small resonant perturbations.

The turbulence was driven with specially designed quasi-stochastic driving on outer scale (with wave numbers in the interval  $k = 2..3.5$ ) with self-correlation time of 2 in code units. The driving worked until stationary state was reached. The scale of the largest coherent eddy in the simulation was around 0.2 of the cube size. This is the outer scale of turbulence  $L = 0.2$ . This largest correlation scale of velocity and magnetic perturbations is determined by nonlinear interaction and is typically less than the driving correlation scale. On the driving scales, i.e.  $k = 2..3.5$  the turbulence is not yet fully developed and the spectrum is distorted, having a characteristic bump, and well-developed turbulence starts with  $k = 5$ . Another definition of outer scale is through anisotropy. One can expect the anisotropy to follow a Goldreich-Sridhar critical balance  $k_{\parallel} = k_{\perp}^{2/3} L^{-1/3}$ . This also lead to the estimate of  $L = 0.2$ <sup>5</sup>, with turbulence being approximately isotropic at  $k = 5$  and approximately 1 : 2 anisotropic at  $k = 40$  for trans-Alfvénic case. At any given time the cube contained large number of independent turbulent realizations ( $> 40$ ). Spectra for one balanced and one imbalanced case are presented on Fig. 1. Further details of the code and simulations can be found in BL09(a,b).

## 2.2. Particle tracing

The electric field in the laboratory frame was obtained through  $E = -[v \times B]/c$  equation, assuming  $v_A/c = 10^{-5}$  (a typical value for the ISM)<sup>6</sup>. The particles were injected randomly through the cube and the trajectories were traced by hybrid Runge-Kutta quality-controlled ODE solver, assuming periodic boundaries for particles as well as fields.

In particular, we solved 6 equations:

<sup>5</sup> Here we omit  $2\pi$  factor normally present in size-wavevector relation, as we normalized cube size to unity.

<sup>6</sup> The velocity was measured in the Alfvénic units and the electric field is in the same units as magnetic field

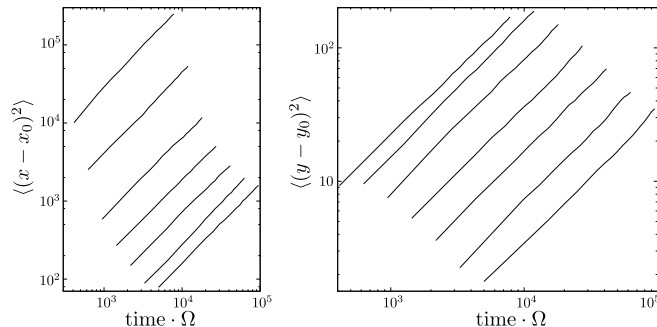


FIG. 2.— Diffusive behavior of the particles in the tracing simulations. For different  $r_L$  we show ensemble-averaged square deviations, which are proportional to time.  $x$  and  $y$  are measured in units of the cube size.

$$\frac{d\hat{\mathbf{u}}}{\hat{s}} = \hat{\gamma}\mathbf{E} + \hat{\mathbf{u}} \times \mathbf{B} \quad (3)$$

$$\frac{d\mathbf{x}}{\hat{s}} = r_L \hat{\mathbf{u}}. \quad (4)$$

Here  $\hat{\mathbf{u}}$  is the normalized space component of the 4-velocity,  $\hat{\mathbf{u}} = \mathbf{u}/\gamma_0$ , where  $\gamma_0$  is the initial particle gamma-factor. Also  $\hat{\gamma} = \sqrt{1/\gamma_0^2 + \hat{\mathbf{u}}^2}$ .  $\hat{s} = (eB_0/mc^2)s$  is a self-time measured in cyclotron frequency units (a gyration frequency in particle's own frame). A particle with  $\mu = 0$  will make a full orbit in  $B_0$  field in  $2\pi$  time. Therefore, we conveniently measure scattering frequency relative to gyration frequency. The measure of initial particle's energy, normalized Larmor radius is expressed as  $r_L = mc^2\gamma_0/eB_0$ . Physically, one can think of  $\gamma_0$  is a measure of relativity of the particle, i.e. for small  $\gamma_0$  we will recover nonrelativistic equations, and for large  $\gamma_0$  – ultra-relativistic equations. At the same time,  $r_L$  is the measure of energy, but with respect to the perpendicular size of the simulation box. In most simulations we took  $1/\gamma_0$  (which enters only in the equation for  $\hat{\gamma}$ ) as zero or close to zero, such as  $10^{-5}$ , this corresponds to ultra-relativistic particles. The  $r_L$  was varied from 0.1 of the cube size to around a grid size. Fig. 2 presents ensemble-averaged square distance vs time for different  $r_L$ . The square distance grows linearly with time, which is expected for diffusive motion.

### 3. EXPECTED CR TRANSPORT PROPERTIES IN MHD TURBULENCE

#### 3.1. Formalism for NLT

We start with explaining QLT which is the theory for resonant interactions: gyroresonance scattering and transit scattering (also called transit time damping, TTD). The resonant condition is  $\omega - k_{\parallel}v\mu = n\Omega$  ( $n = 0, \pm 1, 2, \dots$ ), where  $\omega$  is the wave frequency,  $\Omega = \Omega_0/\gamma$  is the relativistic gyration frequency,  $\mu = \cos\theta$ ,  $\theta$  is the pitch angle of particles. TTD corresponds to  $n = 0$  and it requires compressible perturbations. Most of the gyroresonance contribution comes from  $n = 1$ .

It was demonstrated that scattering by Alfvénic turbulence is substantially suppressed due to its anisotropy (Chandran 2000, YL02). Fig. 3 illustrates why interaction is suppressed. The scattering rate in GS95 turbulence with outer scale of  $L$  and assuming that  $\theta$  is not close to 0 is given by QLT as (YL02):

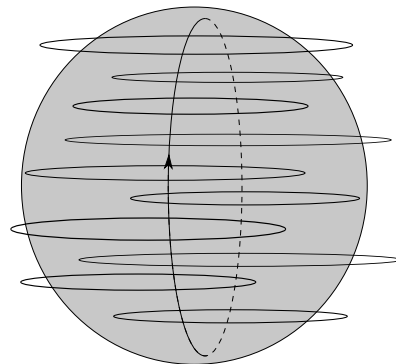


FIG. 3.— Cartoon illustrating that the CR gyroresonance scattering in strongly anisotropic (GS95) turbulence is very ineffective. In perpendicular direction CRs feel many uncorrelated eddies and the interaction averages out.

$$D_{\mu\mu} = \frac{v^{2.5}\mu^{5.5}}{\Omega^{1.5}L^{2.5}(1-\mu^2)^{0.5}}\Gamma[6.5, k_{max}^{-\frac{2}{3}}k_{\parallel,res}L^{\frac{1}{3}}], \quad (5)$$

where  $\Gamma[a, z]$  is the incomplete gamma function,  $k_{max}$  correspond to the dissipation scale of turbulence and  $k_{\parallel,res}v\mu = \Omega$ . The scattering frequency, therefore, is approximately Bohm-like if Larmor radius is of the order of  $L$ , but then falls steeply as  $\Omega^{-1.5}$  and becomes negligible for small energies.

Contrary to QLT which assume that the magnitude of the magnetic field stay constant, NLT relaxes this assumption and allow this quantity to change gradually, adiabatically with respect to particle motion. Due to conservation of adiabatic invariant  $p_{\perp}^2/B$  (see Landau & Lifshits 1975) the pitch angle will gradually vary, resulting in resonance broadening (Völk, 1975). Nonlinear transport (NLT) formalism is based on the replacement of the sharp resonance between waves and particles  $\delta(k_{\parallel}v\mu - \omega \pm n\Omega)$  from QLT to the “resonance function”  $R_n$  (YL08):

$$R_n = \Re \int_0^{\infty} dt e^{i(k_{\parallel}v\mu + n\Omega - \omega)t - \frac{1}{2}k_{\parallel}^2v_{\perp}^2t^2 \left(\frac{\langle \delta B_{\parallel}^2 \rangle}{B_0^2}\right)^{\frac{1}{2}}} \\ = \frac{\sqrt{\pi}}{|k_{\parallel}\Delta v_{\parallel}|} \exp\left[-\frac{(k_{\parallel}v\mu - \omega + n\Omega)^2}{k_{\parallel}^2\Delta v_{\parallel}^2}\right], \quad (6)$$

The width of the resonance function depends on the perturbation strength of the turbulence  $\Delta\mu = \Delta v_{\parallel}/v_{\perp} \simeq \sqrt{\delta B/B} = \sqrt{M_A}$ . For gyroresonance ( $n = \pm 1, 2, \dots$ ) the result depends on whether  $\mu$  is strongly or weakly perturbed by regular field. If  $\mu \gg \Delta\mu$ , the result is similar to QLT, because the exponents in Eq.(6) become close to  $\delta$ -functions. For  $\mu < \Delta\mu$ , however, the result is different. To demonstrate this we can consider the case of  $90^\circ$  scattering. Indeed, if  $\mu \rightarrow 0$ , the resonance happens mostly at  $k_{\parallel,res} \sim \Omega/\Delta v$ , while in QLT  $k_{\parallel,res} \sim \Omega/v_{\parallel} \rightarrow \infty$ . Compared to TTD, however,  $D_{\mu\mu}$  for gyroresonance is still smaller in incompressible case (see Fig. 4) due to anisotropy.

#### 3.2. Scattering in strong MHD turbulence

Assuming the tensor of magnetic perturbations introduced in Cho et al. (2002), which is consistent with the

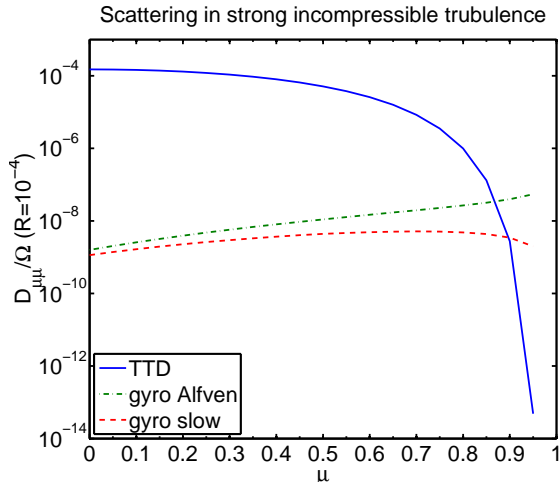


FIG. 4.— Scattering of CRs with  $R = r_L/L = 10^{-4}$  in strong incompressible trans-Alfvénic turbulence. Solid line represents TTD contribution. Dash-dot refers to the gyroresonance with the Alfvén mode while dash line is for the gyroresonance with the slow mode. See eqs 7, also see YL08.

GS95 model, we can calculate scattering from TTD and gyroresonance. Assuming small energies corresponding to Larmor radii much smaller than the outer scale one gets for TTD (YL08):

$$D_{\mu\mu}^T = \frac{\sqrt{\pi} M_A^{7/2} v}{16L} (1 - \mu^2)^{3/2} [-E_1(q\xi_{\parallel}) - e^{-q\xi_{\parallel}}]_1^{\xi_{\parallel, \max}} \times \exp \left[ -\frac{(\mu - v_A/v)^2}{\Delta\mu^2} \right], \quad (7)$$

where  $\xi = kL$ ,  $E_1(\xi) = \int_1^{\infty} dt \exp(-\xi t)/t$  and  $q = (\xi_{\perp, \max} M_A^2)^{-2/3}$ .

Fig. 4 displays the pitch angle diffusion coefficients resulting from TTD scattering and gyroresonance (YL08). We see that gyroresonance is mostly subdominant, however at small pitch angles TTD is inefficient and gyroresonance dominates.

#### 4. MEASUREMENTS OF SCATTERING

$D_{\mu\mu}$  scattering property was measured in the tracing experiments where an ensemble of particles with the same  $r_L$  (energy) and a particular  $\mu_0$  were traced by a certain time. This time was determined by the condition that the rms of deviations of  $\mu$  is small (i.e. 0.1-0.01). Then the curves of the ensemble-averaged  $\langle (\mu - \mu_0)^2 \rangle$  were fitted with a linear curve, and so  $D_{\mu\mu}$  was obtained. The  $D_{\mu\mu}$  for trans-Alfvénic case is presented on Fig. 5. For sub-Alfvénic case we noticed that there were very few  $90^\circ$  scattering events. This will be explained in the next section.

As we see from Fig. 5 the measurement of scattering frequency is *incompatible* with QLT. The scattering frequency normalized to the gyration frequency is proportional to the Larmor radius i.e. it is constant with energy (as  $\Omega r_L = v \approx c$ ). It would be reasonable to assume then that particles of all energies scatter on the same objects, magnetic bottles, formed by large scale slow-mode perturbations. The same result could be obtained from NLT, taking into account  $\Delta\mu \sim \mu$  in strong turbulence. At larger energies scattering becomes less efficient i.e.

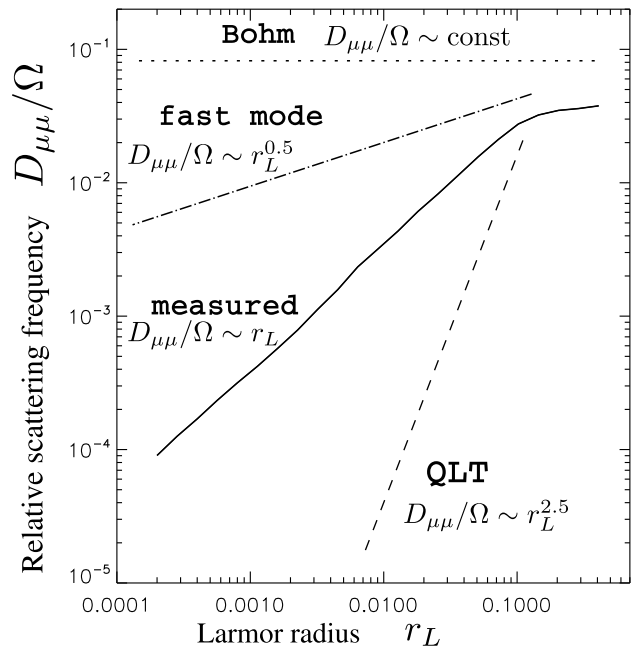


FIG. 5.— Dimensionless CR scattering coefficient  $D_{\mu\mu}/\Omega$  for the case of  $\mu = 0.71$  vs Larmor radius  $r_L$  expressed in cube size units (solid line). We suppose that it is dominated by magnetic bottles formed by slow mode, this is why  $D_{\mu\mu}$  (dimensional scattering frequency) is almost constant, i.e. independent on particle’s energy. For comparison, we plot various theoretical predictions: QLT prediction for Alfvén and slow mode (dashed); QLT prediction for fast mode (dot-dashed), note that in our data fast mode was absent, so this line is only for reference; hypothetical Bohm scattering or maximally efficient scattering (dotted).

high energy particles “feel” less mirrors. This transition happen at around  $r_L/L \approx 0.1$ .

Due to the lack of outer scale, the  $D_{\mu\mu}$  for sub-Alfvénic case is supposed to be QLT-like and very small. As such it was severely contaminated by numerical error, in particular, fields interpolation error and was not obtained in this study.

#### 5. MEASUREMENTS OF SPACE DIFFUSION

The measurements of space diffusion  $D_{xx}$  and  $D_{yy}$  were more straightforward than the measurements of  $D_{\mu\mu}$  because we did not limit the integration time as in the previous section. Therefore, we integrated for as long as it took for the  $\langle (x - x_0)^2 \rangle$  and  $\langle (y - y_0)^2 \rangle$  to show good diffusive linear dependence with time. Those integration times turned out to be very long, so the particles crossed outer-scale of turbulence for many times. Therefore these measurements correspond to diffusion on outer scale and not to “sub-diffusion” (see, e.g., YL08). Moreover, we measured diffusion with respect to some global frame of reference, determined by the global mean magnetic field. Therefore, our measurements do not necessarily correspond to theories that measure “parallel” or “perpendicular” diffusion with respect to the magnetic field lines.

Also, we were only able to obtain the *lower limit* of  $D_{xx}$  for *sub-Alfvénic* case due to the very low  $90^\circ$  scattering frequency. This was manifested by the fact that as we increased the precision of the code, the  $D_{xx}$  increased and did not show convergence. This very low scattering frequency has to do with what we discussed earlier – the lack of larger scale perturbations in sub-Alfvénic cubes.

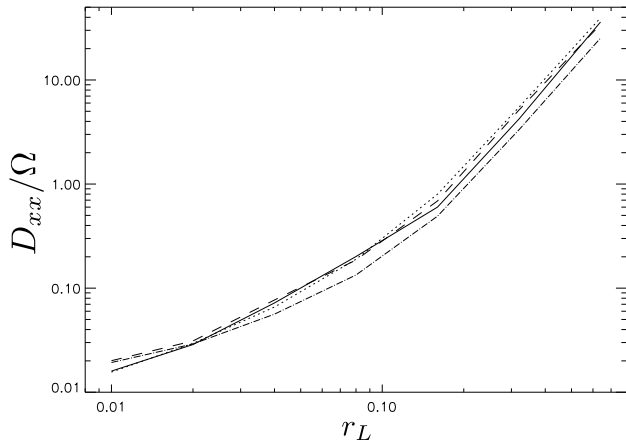


FIG. 6.— Parallel diffusion in trans-Alfvénic case. Solid – “balanced”, dotted – “slightly imbalanced” dashed – “strongly imbalanced”, dot-dashed – “very strongly imbalanced” (see BL09a for more details).

In this case, since  $\Delta\mu < \mu$ , the resonance function becomes narrow so that marginal interaction is available at  $90^\circ$ <sup>7</sup>. In other words, in the absence of the large-scale perturbations, which are normally present in nature, but absent in our sub-Alfvénic cubes, the  $90^\circ$  scattering becomes problematic and parallel diffusion is replaced by ballistic propagation along mean field. At the same time, this suggests that QLT (resonant scattering) can not be used for low energy particle scattering, as large scales contribute more than the resonant scales.

As the mean magnetic field was along ‘x’ axis, our  $D_{xx}$  coefficient correspond to “parallel diffusion”, while  $D_{yy}$  correspond to “perpendicular diffusion”. This correspondence, however, is tentative, since most theories predict “parallel” or “perpendicular” diffusion as happening with respect to the local magnetic field lines. We nevertheless will use terms “parallel” and “perpendicular” to  $D_{xx}$  and  $D_{yy}$ . We also claim that the measurement of the diffusion with respect to the global reference frame has more practical importance and is easier applicable to the results of observations.

### 5.1. Parallel diffusion

The results for parallel diffusion for trans-Alfvénic case are presented on Fig. 6. Along with standard ‘balanced’ MHD turbulence case (presented by solid line) we calculated this diffusion coefficient for simulations with different degree of imbalance, using datacubes from simulations of Beresnyak & Lazarian 2009a. As the aforementioned paper (along with the earlier study Beresnyak & Lazarian 2008) are the first high-resolution simulations of stationary strong imbalanced turbulence, it is important<sup>8</sup> to numerically study the scattering coefficient, even more so when the theory is lacking.

As we see from Fig. 6 at small energies  $D_{xx}/\Omega$  is linearly proportional to  $r_L$ , i.e. as in the case with  $D_{\mu\mu}$  the scattering frequency is independent of energy. At higher energies it becomes proportional to the square of

<sup>7</sup> The case with sub-Alfvénic turbulence may be viewed as a transition to the QLT case, where the resonance function shrinks to  $\delta$  function and there is no TTD resonance at  $90^\circ$

<sup>8</sup> For example, Solar Wind exhibit imbalanced turbulence up to distances of around 1 AU, with perturbations coming from the Sun being prevalent over backward-going perturbations.

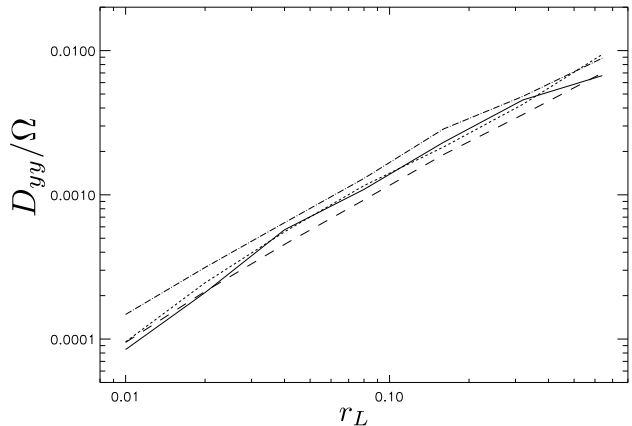


FIG. 7.— Perpendicular diffusion in sub-Alfvénic case  $\delta B/B = 1/10$

$r_L$ . This is again consistent with the behavior of  $D_{\mu\mu}/\Omega$  from Fig. 5, i.e. that at high energies  $D_{\mu\mu} \sim \Omega$  and as  $D_{xx} \sim 1/D_{\mu\mu}$ ,  $D_{xx}/\Omega \sim 1/\Omega^2 \sim r_L^2$ . The transition happens at  $r_L/L \approx 0.1$ , same as in Fig. 5. So we conclude that the measurements of  $D_{xx}$  and  $D_{\mu\mu}$  are consistent with each other. A note of caution towards direct comparison of these two measurements is due, however. In the measurement of  $D_{xx}$  we did not control particle’s energy, which could undergo changes during the long integration times of  $D_{xx}$  measurement.  $D_{\mu\mu}$ , however, was measured during short times, and as electric field was assumed small (smaller than  $B$  by a factor of  $v_A/c \approx 10^{-5}$ ), there wasn’t significant energy change during this short time. This can explain why the transition between two regimes of scattering is more sharp of Fig. 5 rather than Fig. 6. Also, as we mentioned previously,  $D_{xx}$  is the diffusion coefficient measured in the *global reference frame*, while  $D_{\mu\mu}$  defines pitch-angle scattering with respect to the local field direction.

Fig. 6 also shows that the diffusion coefficient is pretty independent on the degree of imbalance, indicating that the trans-Alfvénic imbalanced turbulence has approximately as many magnetic bottles as its balanced counterpart. This is consistent with the assumption that only large-scale perturbations significantly contribute to scattering. Indeed, in the imbalanced simulations of BL09a the outer-scale magnetic field was determined primarily by the stronger Elsasser component and has similar structure and magnitude and outer-scale magnetic field in balanced simulations.

### 5.2. Perpendicular diffusion

Perpendicular diffusion coefficients are presented on Figs. 7, 6. As to various models, regimes and terminology of perpendicular diffusion we refer the reader to YL08 and refs therein. Let us first interpret the measurements in the sub-Alfvénic case. We chose initial particle’s pitch angle to be  $45^\circ$ . As we discussed earlier, due to the particular choice of the data, there wasn’t any  $90^\circ$  scattering in this case. I.e. particles moved ballistically along ‘x’ axis, but their trajectories diffused from the center due to magnetic field wandering. As suggested by Fig. 7 the dependence of this plot is almost linear, i.e.  $D_{yy}/\Omega \sim r/L$  or  $D_{yy}$  is independent of energy.

In the three-dimensional turbulence, field lines are diverging away due to shearing by Alfvén modes (see

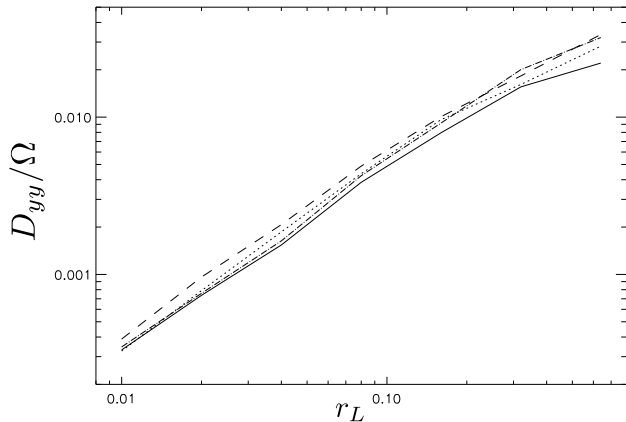


FIG. 8.— Perpendicular diffusion in trans-Alfvénic case  $\delta B/B = 1$ .

Lazarian & Vishniac 1999, Narayan & Medvedev 2002). Most recently the diffusion in magnetic fields was considered for thermal particles in Lazarian (2006, 2007). The cross-field transport can result from the deviations of field lines at small scales, as well as field line random walk at large scale.

If we assume that the particle follow magnetic field line and is diffused only by the outer-scale magnetic field wandering, the perpendicular diffusion can be expressed as  $D_{yy}/(L^2\Omega) \approx 2^{-1/2}(L_{tr}/L)^2 \cdot (L/L_{\parallel}) \cdot (r_L/L)$ , where  $L_{\parallel}$  is the outer parallel scale (which is 10 times bigger than  $L$  in our sub-Alfvénic simulation),  $1/\sqrt{2}$  is the cosine of pitch angle and  $L_{tr}$  is the distance the particle is deflected when it travels  $L_{\parallel}$  along the field line (see eq. (26) in YL08). We would expect  $L_{tr}$  to be close to  $L$ . From the fit of Fig. 7 we derive  $L_{tr}/L \approx 0.92$  which is fairly close, considering the uncertainty in  $L$ . Using the same argumentation we obtain  $L_{tr}/L \approx 0.53$  from the fit of Fig. 6 which is short of what we expected. This is an indication that the impediment of travel in parallel direction which is present in trans-Alfvénic case due to  $90^\circ$  scattering decreases diffusion in perpendicular direction. We stop with this conclusion, as there is clearly not enough data for a detailed comparison with different models in YL08.

## 6. DISCUSSION

In this paper we numerically measured diffusion coefficients that arise when particle propagates in a turbulent magnetic fields. Unlike previous studies, we used realistic fields obtained in a three-dimensional simulations of MHD turbulence. The focus of this paper was the incompressible case, where fast magnetosonic mode is absent. The earlier QLT calculations presumed that particle scattering is negligible in this case, as the perturbations are extremely anisotropic with respect to the mean field. We figured that QLT is not applicable when the magnitude of the magnetic field is strongly perturbed, and that another approach called NLT has to be adopted (YL08). NLT allows relatively efficient scattering through TTD as the particle’s pitch angle changes adiabatically and makes possible for  $90^\circ$  scattering. One can interpret this as scattering through large-scale magnetic mirrors.

We confirmed this picture of mirrors by measuring scattering frequency which is independent on energy, for small energies. We also studied spacial diffusion which,

in the case of parallel diffusion is related to scattering frequency. The case of perpendicular diffusion is more complicated. We showed that if particles do not scatter in parallel direction, the perpendicular diffusion is mostly due to magnetic field line wandering. This case could be unphysical though, as the absence of parallel scattering was due to the absence of larger scales in the simulation. In the case when parallel diffusion was operating, the perpendicular diffusion was reduced. At this point, however, we don’t have enough data to distinguish between different models of perpendicular diffusion.

The special attention should be brought to the astrophysical interpretation of scattering in the imbalanced turbulence. Figs. 6-8 indicate that the scattering is similar to the balanced case. This is qualitatively and quantitatively agree with the picture that was presented in this paper, namely that in the incompressible case most of the scattering will come from the outer scale of turbulence and most of the perpendicular diffusion will come from the field wandering on the outer scale. This fact, however, does not mean that the scattering in the astrophysical objects will be the same regardless of the degree of imbalance. The key to understand this is to understand the nature of our MHD simulations. In these simulations we kept the fluctuation amplitude and the anisotropy *controlled on outer scale*, the physically all-important *dissipation rate*, however, varied greatly depending on the degree of imbalance. In astrophysics, turbulence is caused by the sources of kinetic energy, such as stellar and AGN jets, stellar winds interacting with the ISM, supernovae, the Sun creating perturbations in the solar wind. Turbulent dissipation will have to balance this influx of energy, however, dissipation depends greatly on the degree of imbalance, therefore, in a situation with a constant influx of energy imbalanced turbulence will have much larger perturbation amplitudes, which will result in a much more efficient scattering. With respect to relation between dissipation rate and perturbation amplitude we refer to the imbalanced turbulence model presented in Beresnyak & Lazarian 2008, as the most realistic model to-date, and the simulations in BL09a. A word of caution towards directly using these results is due, however. Aforementioned model and the simulations in BL09a describe *stationary* imbalanced turbulence. However, as we learned from these studies, the time of establishment of stationary state greatly increases with larger imbalances. As astrophysical processes are usually transient, it is possible that in a situation with large imbalance the stationary state will not be achieved. The *stationary* imbalanced turbulence could still be used to infer the properties of small-scale fluctuations, as timescales are smaller, but, as we saw in this study, large scales are important for scattering. This problem will be solved by the models of transient and inhomogeneous imbalanced turbulence, although at present such models are still in their infancy (see, e.g., the Appendix in BL09a). We are optimistic, however, that the properties of CR scattering in realistic astrophysical objects that feature imbalanced turbulence, such as solar and stellar winds, AGN jets and many others will be figured out.

Although NLT prediction for nonresonant mirror scattering by incompressible turbulence puts a lower limit on CR scattering, in most realistic astrophysical circumstances, there several mechanisms that could compete

with it. If the fast mode is present and have a sufficient amplitude in the range of scales corresponding to Larmor radii of low-energy CRs, those CRs will be scattered primarily due to fast mode (YL04). Also, if CRs have large density gradients and tend to stream in a particular direction, such as CRs escaping the Galaxy, or CRs streaming in front of the supernovae shock, the back-reaction to MHD fluid will be important. Speaking of turbulence, in this paper we considered generic astrophysical turbulence driven on large scales. Other types of astrophysical turbulence are often important for scattering and acceleration. This includes MRI turbulence (see, e.g., Hawley et al, 2001), and turbulence generated by CR-MHD fluid interaction in supernova shocks (see, e.g., Beresnyak et al 2009 and ref. therein).

Stochastic acceleration by MHD turbulence was not studied here as the correct calculation requires *time-dependent* MHD fields, so that simulations of turbulence are integrated at the same time as particles propagate. This will be a matter of a future research.

AB is supported by ICECUBE project. AB is grateful to TeraGrid project for providing him with computational resources. HY is supported by Arizona Prize Fellowship. AL acknowledges the NASA grant X5166204101, the NSF grant ATM-0648699, as well as the NSF Center for Magnetic Self-Organization in Laboratory and Astrophysical Plasmas.

#### REFERENCES

- Bell, A. R. 1978, MNRAS, 182, 147  
 Beresnyak, A., Jones, T. W., & Lazarian, A., 2009, ApJ, 707, 1541,  
 Beresnyak, A., & Lazarian, A. 2006, ApJ, 640, L175  
 Beresnyak, A., & Lazarian, A. 2008, ApJ, 682, 1070  
 Beresnyak, A., & Lazarian, A. 2009a, ApJ, 702, 460 (BL09a)  
 Beresnyak, A., & Lazarian, A. 2009b, ApJ, 702, 1190 (BL09b)  
 Bieber, J. W., Smith, C. W., & Matthaeus, W. H. 1988, ApJ, 334, 470  
 Biskamp, D., 2003, *Magnetohydrodynamic Turbulence*, Cambridge: Cambridge Univ. Press.  
 Boldyrev, S. 2005, ApJ, 626, L37  
 Boldyrev, S. 2006, Phys. Rev. Lett. 96, 115002  
 Brunetti, G. & Lazarian, A. 2007, MNRAS, 378, 245  
 Chandran, B. 2000, Phys. Rev. Lett., 85(22), 4656  
 Cho, J. & Lazarian, A. 2002, Phys. Rev. Lett., 88, 245001  
 Cho, J. & Lazarian, A. 2003, MNRAS, 345, 325  
 Cho, J., Lazarian, A. & Vishniac, E.T. 2002, ApJ, 564, 291  
 Cho, J., & Vishniac, E. 2000, ApJ, 539, 273  
 Dupree, T. H., 1966, Phys. Fluids, 9, 1773  
 Felice, G. M. & Kulsrud, R. M., 2001, ApJ, 553, 198  
 Forman M. A., Jokipii, J. R., & Owens, A. J. 1974, ApJ, 192, 535  
 Galtier, S., Nazarenko, S.V., Newel, A.C., Pouquet, A., J. Plasma Phys. 2000, 63, 447  
 Giacalone, J., & Jokipii, J. R. 1999, ApJ, 520, 204.  
 Gogoberidze, G. 2007, Phys. Plasma, 14, 22304  
 Goldreich, P. & Sridhar, H. 1995, ApJ, 438, 763  
 Goldstein, M., 1976, ApJ, 204, 900  
 Hawley, J.F., Balbus, S.A., Stone, J.M. 2001, ApJ, 554, L49  
 Jokipii, J. R. 1966, ApJ, 146, 480  
 Jokipii, J. R. & Parker, E. N., 1969, ApJ, 155, 777  
 Jones, F. C., Birmingham, T. J., Kaiser, T. B., 1973, ApJ, 180, L139  
 Jones, F. C., Birmingham, T. J., Kaiser, T. B., 1978, Phys. Fluids, 21, 347  
 Kóta, J., & Jokipii, J. R. 2000, ApJ, 531, 1067  
 Krymsky, G.F. 1977, Sov. Phys. Dokl. 23, 327  
 Kulsrud, R. & Pearce, W.P. 1969, ApJ, 156, 445  
 Landau, L. D. & Lifshitz, E. M., 1975, *The classical theory of fields*, 4th rev. English ed., Pergamon Press  
 Lazarian, A., 2007, in "Turbulence and Nonlinear Processes in Astrophysical Plasmas", eds. D. Shaikh and P. Zank, AIP 978, p.58  
 Lazarian, A., 2006, ApJ, 645, L25  
 Lazarian, A. & Vishniac, E. 1999, ApJ, 517, 700L  
 Lithwick, Y. and Goldreich, P. 2001, ApJ, 562, 279  
 Maron, J. & Goldreich, P. 2001, 554, 1175  
 Matthaeus, W., H., Qin, G., Bieber, J. W., & Zank, G. P., 2003, ApJ, 590, L53  
 Mace, R. L., Matthaeus, W. H., & Bieber, J. W. 2000, ApJ, 538, 192  
 Malkov, M.A., Drury, L.O'C. 2001, Rep. Prog. Phys. 64, 429  
 Müller, W. C., & Biskamp, D., 2000, Phys. Rev. Lett. 84(3), 475  
 Narayan, R., & Medvedev, M., 2001, ApJ, 562, 129L  
 Owens, A. J. 1974, ApJ, 191, 235  
 Qin, G., Matthaeus, W. H. & Bieber, J. W. 2002, ApJ, 578, L117  
 Schlickeiser, R. 2002, *Cosmic Ray Astrophysics* (Springer-Verlag: Berlin Heidelberg)  
 Skilling, J. 1975, MNRAS, 172, 557  
 Völk, H. J. 1973, Ap&SS, 25, 471  
 Völk, H. J. 1975, Rev. Geo. Space Phys., 13, 547  
 Yan, H., & Lazarian, A., 2002, Phys. Rev. Lett, 34, 1292 (YL02)  
 Yan, H., & Lazarian, A., 2004, ApJ, 614, 757 (YL04)  
 Yan, H., & Lazarian, A., 2008, ApJ, 673, 942 (YL08)